Mutual Coherence and Interference in Resonance Fluorescence

P. Kochan,[1] H. J. Carmichael,[1] P. R. Morrow,[2] and M. G. Raizen[2]
[1]*Department of Physics, Chemical Physics Institute, and Institute of Theoretical Science, University of Oregon, Eugene, Oregon 97403*
[2]*Department of Physics, University of Texas at Austin, Austin, Texas 78712*
(Received 13 February 1995)

We study theoretically the interference of the resonance fluorescence from two atoms coupled to an optical cavity mode. Atom-atom correlations induced by the cavity alter the fringe visibility, which provides a measurement of collective atomic behavior. We use quantum trajectories to explain the loss of mutual coherence for strong excitation and propose a phase-selective measurement to partially restore the coherence. A "which-path" explanation for the loss of coherence is also discussed.

PACS numbers: 42.50.Ar, 42.50.Dv

The scattering of light by an atom driven near resonance is one of the most elementary physical processes. Despite the outward appearance of simplicity, however, a remarkably complex phenomenon was revealed by studies of the spectrum and statistics of the emitted radiation [1]. Given the attention the subject subsequently received, it is perhaps surprising that the coherence properties of resonance fluorescence still have not been studied fully experimentally. For example, for many years no experiments were performed on the mutual coherence of two radiating atoms. Here, first-order coherence must be measured using interference, as in the Young two-slit experiment, which requires the isolation and localization of the atoms—clearly a major experimental challenge. With recent advances in ion trapping technology [2], such experiments are now possible and a Young two-slit experiment with trapped and laser-cooled ions was recently reported [3]. Based on these first results it is now important to study first-order coherence in different excitation regimes. For example, for weak excitation the scattering is predominantly elastic and the interference fringe visibility should be unity (to the extent that ion motion can be neglected). Under stronger excitation, inelastic scattering increasingly occurs and the interference pattern is expected to disappear. In this Letter we present some ideas concerning the latter regime. We report three main results: (i) We analyze a modified version of the two-slit experiment in which the atoms are coupled through a mode of the field in an optical cavity and propose that Young's interference can be used to detect the collective character of the emission into the cavity mode. (ii) We present a quantum trajectory analysis [4] of the loss of visibility with increasing excitation strength in free space. The analysis points to a method for partially restoring the visibility in a cavity by conditioning its measurement on the detection of photons transmitted through the cavity mirrors. (iii) We analyze the role of "which-path" information on the loss of visibility in free space. We show that which-path information is provided by the internal state (dressed state) of the atoms; a strongly coupled cavity can track the internal state [as a quantum nondemolition (QND) detector] so that a conditioned measurement restores the full visibility.

A model suitable for addressing all of these issues consists of a pair of two-state atoms, coupled to a mode of an optical cavity, and driven by coherent light of amplitude $\mathcal{E}$. The atoms, cavity mode, and driving field are all on resonance. One detector, A (Fig. 1), records the interference pattern and a second detector, B, is used to make conditioned measurements. For simplicity we assume that the atoms couple to the cavity mode with the same coupling constant $g = (\mu/\hbar)\sqrt{\hbar\omega/2\epsilon_0 V}$, where μ is the dipole moment and V is the cavity mode volume. The atoms are at rest, separated by a distance $s \gg \lambda$, where λ is the optical wavelength; thus, in the absence of the cavity they radiate independently. γ_I is the cavity-inhibited spontaneous emission rate out the sides of the cavity and 2κ is the photon decay rate from the cavity mode. The model is described by the master equation

$$\begin{aligned}\dot{\rho} = &[(\mathcal{E} + g\hat{a}^\dagger)(\hat{\sigma}_- + \hat{\Sigma}_-) - (\mathcal{E} + g\hat{a})(\hat{\sigma}_+ + \hat{\Sigma}_+), \rho] \\ &+ \kappa(2\hat{a}\rho\hat{a}^\dagger - \hat{a}^\dagger\hat{a}\rho - \rho\hat{a}^\dagger\hat{a}) \\ &+ (\gamma_I/2)(2\hat{\sigma}_-\rho\hat{\sigma}_+ - \hat{\sigma}_+\hat{\sigma}_-\rho - \rho\hat{\sigma}_+\hat{\sigma}_-) \\ &+ (\gamma_I/2)(2\hat{\Sigma}_-\rho\hat{\Sigma}_+ - \hat{\Sigma}_+\hat{\Sigma}_-\rho - \rho\hat{\Sigma}_+\hat{\Sigma}_-), \quad (1)\end{aligned}$$

where ρ is the density operator (in the interaction picture), $\hat{\sigma}_+$ ($\hat{\Sigma}_+$) and $\hat{\sigma}_-$ ($\hat{\Sigma}_-$) are dipole raising and lowering operators for the first (second) atom, and $\hat{a}^\dagger$ and $\hat{a}$ are creation and annihilation operators for the cavity mode. Free-space conditions [3] are obtained with $g = \kappa = 0$ and $\gamma_I = \gamma$, where γ is the Einstein A coefficient.

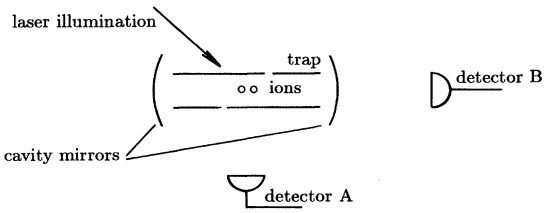

FIG. 1. Schematic representation of the physical model.

0031-9007/95/75(1)/45(4)$06.00

The electric field operator at detector A is proportional to the sum of the atomic dipole operators, and the mean intensity of the interference pattern may be written as

$$I(x) = \langle \hat{\sigma}_+ \hat{\sigma}_- + \hat{\Sigma}_+ \hat{\Sigma}_- \rangle + \langle \hat{\sigma}_+ \hat{\Sigma}_- + \text{H.c.} \rangle \cos\theta , \tag{2}$$

where $\theta = 2\pi x s/\lambda R$; $R \gg s$ is the distance from the atoms to the detector, and x is a coordinate which locates the detector along a line perpendicular to the propagation direction of the scattered light. The visibility calculated from Eq. (2) is

$$V = \langle \hat{\sigma}_+ \hat{\Sigma}_- + \text{H.c.} \rangle / \langle \hat{\sigma}_+ \hat{\sigma}_- + \hat{\Sigma}_+ \hat{\Sigma}_- \rangle . \tag{3}$$

In free space the atoms radiate independently and the average $\langle \hat{\sigma}_+ \hat{\Sigma}_- \rangle$ in the numerator of Eq. (3) may be factorized. The steady-state solution to standard optical Bloch equations then gives

$$V = \langle \hat{\sigma}_+ \rangle \langle \hat{\Sigma}_- \rangle / p_+ = [1 + 8(\mathcal{E}/\gamma)^2]^{-1}, \tag{4}$$

where p_+ is the excited state probability for each atom. The visibility is unity for weak excitation and decreases monotonically with increasing excitation strength.

When coupled through the cavity mode the atoms do not radiate independently and the factorization leading to Eq. (4) does not hold. The visibility (3) then provides a measure of the atom-atom correlations. We have calculated the visibility in steady state by solving the master equation (1) numerically using the states $|\xi, \Xi, n\rangle$ as a basis, where $\xi = +$ or $-$ ($\Xi = +$ or $-$) denotes the state of the first (second) atom, and n is the number of photons in the cavity mode. All results were obtained for steady-state photon numbers less than unity, permitting a truncation of the basis at $n = 2$.

The results are plotted in Fig. 2 (open circles and squares). Figure 2(a) shows the visibility as a function of $\mathcal{E}/\gamma_I$ for direct comparison with Eq. (4) (dashed curve). In Fig. 2(b) the visibility is plotted as a function of $\mathcal{E}'/\gamma_I'$, where $\gamma_I' = \gamma_I + 2g^2/\kappa$ and $\mathcal{E} = \mathcal{E}'\{1 + \beta[1 + 8(\mathcal{E}'/\gamma_I')^2]^{-1}\}$; $\beta = 2g^2/\gamma_I'\kappa$. This rescaling of the driving-field axis is appropriate in the bad-cavity limit ($2\kappa/\gamma_I \longrightarrow \infty$). It accounts for two cavity effects which are not related to atom-atom correlations: cavity enhancement of the spontaneous emission rate ($\gamma_I \rightarrow \gamma_I'$), and reduction of the mean field amplitude driving each atom due to radiation from the neighboring atom ($\mathcal{E} \rightarrow \mathcal{E}'$). In the absence of atom-atom correlations these effects lead to Eq. (4) with $\mathcal{E}/\gamma$ replaced by $\mathcal{E}'/\gamma_I'$ [upper dashed curve in Fig. 2(b)]. Departures from this behavior provide a measure of the atom-atom correlations. It may be shown (for $2\kappa/\gamma_I \rightarrow \infty$) that with the correlations included, Eq. (4) holds with $\mathcal{E}/\gamma$ replaced by $\mathcal{E}/\gamma_I'$. Putting $\beta = 1$ in this expression sets an upper bound on the correlation effects [lower dashed curve in Fig. 2(b)].

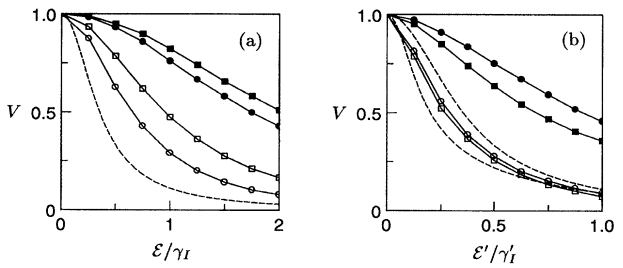

FIG. 2. Fringe visibility as a function of driving field amplitude for $\gamma_I/\kappa = 0.2$. Circles (squares) mark results for $g/\kappa = 0.283$ (0.4); open (filled) markers show results obtained without (with) the phase selection of Eq. (7). The dashed curves are plotted from Eq. (4) (see text).

Consider now a quantum trajectory analysis of the scattering process in free space. In quantum trajectory theory [4], the intensity $I(x)$ is calculated as the time average of the instantaneous, conditioned intensity

$$I_c(x,t) = p_+(t) + P_+(t) + 2z(t)Z(t)\cos\theta , \tag{5}$$

where $p_+(t) = \langle \psi_c(t)|\hat{\sigma}_+\hat{\sigma}_-|\psi_c(t)\rangle$ is the conditioned probability for the first atom to be in the excited state and $z(t) = \langle \psi_c(t)|\hat{\sigma}_-|\psi_c(t)\rangle$ is the (real) conditioned dipole expectation of the first atom [$P_+(t)$ and $Z(t)$ are similarly defined]; $|\psi_c(t)\rangle$ is the conditioned state—a pure state, conditioned on the photoelectric counting records of two imaginary detectors, one monitoring the *imaged* radiation from each of the atoms. [Since detector A collects a negligible fraction of the scattered light, it may be neglected when conditioning the state.]

The decrease in visibility with increasing excitation strength is explained by the evolution of the conditioned dipole expectations $z(t)$ and $Z(t)$. As illustrated in Fig. 3, each grows and collapses back to zero in repeated cycles as the scattering process proceeds. Because the collapse times are statistical (and independent) the cycles are not in phase. For weak excitation, however, $z(t)$ and $Z(t)$ are both negative, since the conditioned Bloch vectors never reach the north pole before suffering a collapse. For sufficiently strong excitation, on the other hand, Rabi oscillations carry the Bloch vectors over the north pole. It is then possible to find one in the eastern hemisphere and the other in the west. In this configuration, $z(t)$ and $Z(t)$ have opposite signs and the conditioned interference pattern [Eq. (5)] is phase shifted by π. Through this

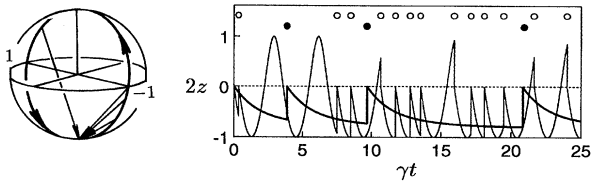

FIG. 3. Quantum trajectory evolution of the first atom in free-space resonance fluorescence: $\mathcal{E}/\gamma = 0.2$ (heavy line) and $\mathcal{E}/\gamma = 1.0$ (light line). The photon emission times are marked by dots. The Bloch sphere illustration shows the first four collapses along the trajectory for $\mathcal{E}/\gamma = 1.0$.

mechanism the visibility of the time average of $I_c(x,t)$ is reduced. (The magnitude of the conditioned interference pattern fluctuates along with the phase. Both fluctuations reduce the time-averaged visibility.)

This explanation provides more than a pleasing picture. It directs us to a measurement scheme in a cavity which partially restores the visibility. The intuitive logic is as follows: The field inside the cavity will be larger (smaller) when $z(t)$ and $Z(t)$ are in phase (out of phase). Let us therefore record a count at detector A, only if it is preceded by a count at detector B. In this way we select against times when the conditioned interference pattern is phase shifted by π—the visibility should increase.

We have calculated visibilities numerically from the phase-selected interference pattern

$$I_s(x) = \int_0^T dt\, I_c(x,t)S(t) \Big/ \int_0^T dt\, S(t), \qquad (6)$$

where $S(t)$ accomplishes the selection; it is unity if a cavity emission occurred in the interval $(t - 2\kappa^{-1}, t]$ and zero otherwise. $I_c(x,t)$ is given by Eq. (2) with the quantum expectations taken with respect to the conditioned state $|\psi_c(t)\rangle$ rather than the density operator ρ. The filled circles and squares in Fig. 2 show the phase-selected visibilities; they are larger by as much as a factor of 4.

To show how our intuitive logic is realized by the quantum trajectory, the evolution of $z(t)$ and $Z(t)$ is illustrated in Fig. 4, with the cavity emission times marked above the figure and the times of the atomic scattering events beneath. Note that, contrary to the intuitive logic, the logic of the quantum trajectory is argued in an *a posteriori* fashion: Conditioned on a cavity emission, the quantum trajectory evolution works to bring the conditioned dipole expectations into phase and establish the correlation we expect; the dipole expectations are not in phase before the cavity emission.

Our final topic is the role of which-path information, where we begin once again by considering the free-space case: Is the loss of visibility predicted by Eq. (4) required, quantum mechanically, because which-path information is available, or do the quantum trajectories of Fig. 3 merely describe a prosaic dephasing process? The answer to this question is surprisingly involved. It is complicated by the fact that strong-field resonance fluorescence is not a one-photon scattering process, with a known initial state for the photon and scatterers. Most importantly, the state of the atoms prior to each scattering event is not known. For weak excitation the following is known: to a good approximation it is the atomic ground state—the state to which the atoms return after a scattering event. For strong excitation, however, the state of the atoms depends on the history of a multiphoton scattering process in a way we now hope to make clear.

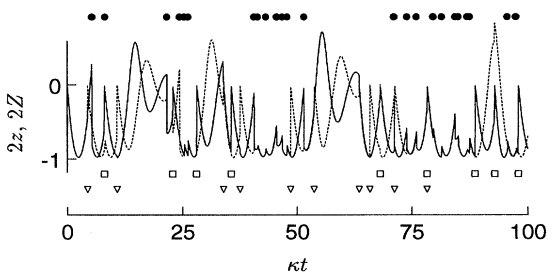

FIG. 4. Typical evolution of the conditioned dipole expectation values for $\mathcal{E}/\gamma_l = 1.0$, $\gamma_l/\kappa = 0.2$, and $g/\kappa = 0.4$.

The possibility of acquiring which-path information lies with the fact that detector A collects only a very few of the scattered photons. Perhaps which-path information can be obtained from the photons that are not collected by detector A. The clearest picture is obtained in the strongly saturated regime where the visibility given by Eq. (4) is essentially zero. It is convenient to introduce the dressed states $|u\rangle$ ($|U\rangle$) and $|l\rangle$ ($|L\rangle$), eigenstates of the Hamiltonian $i\hbar\mathcal{E}(\hat{\sigma}_- - \hat{\sigma}_+)$ [$i\hbar\mathcal{E}(\hat{\Sigma}_- - \hat{\Sigma}_+)$] with energies $+\hbar$ and $-\hbar\mathcal{E}$. Writing

$$\hat{\sigma}_- = -i(\hat{u} - \hat{l} + \hat{d}_+ - \hat{d}_-)/2,$$
$$\hat{\Sigma}_- = -i(\hat{U} - \hat{L} + \hat{D}_+ - \hat{D}_-)/2, \qquad (7)$$

with $\hat{u} = |u\rangle\langle u|$, $\hat{l} = |l\rangle\langle l|$, $\hat{d}_- = |l\rangle\langle u|$, $\hat{d}_+ = |u\rangle\langle l|$, and similar definitions for $\hat{U}$, $\hat{L}$, $\hat{D}_-$, and $\hat{D}_+$, we may then express the conditioned intensity (5) in the form

$$\begin{aligned} 4I_c(x,t) = {} & |\langle u,U|[\hat{u} + \hat{d}_+ + e^{-i\theta}(\hat{U} + \hat{D}_+)]|\psi_c(t)\rangle|^2 \\ & + |\langle l,L|[\hat{l} + \hat{d}_- + e^{-i\theta}(\hat{L} + \hat{D}_-)]|\psi_c(t)\rangle|^2 \\ & + |\langle u,L|[\hat{u} + \hat{d}_+ - e^{-i\theta}(\hat{L} + \hat{D}_-)]|\psi_c(t)\rangle|^2 \\ & + |\langle l,U|[\hat{l} + \hat{d}_- - e^{-i\theta}(\hat{U} + \hat{D}_+)]|\psi_c(t)\rangle|^2. \end{aligned} \qquad (8)$$

This result is written as a transition probability summed over the final states $|u,U\rangle$, $|l,L\rangle$, $|u,L\rangle$, and $|l,U\rangle$. The initial state $|\psi_c(t)\rangle$ is a superposition of the same four states, three of which contribute nonzero amplitudes in each term of Eq. (8). Thus, there are 12 transitions to consider when a photon is recorded by detector A.

The situation is complicated by the fact that the transition amplitudes can interfere. The difficulty is overcome by making the secular approximation. For strong excitation, the $|u,U\rangle$ and $|l,L\rangle$ components of $|\psi_c(t)\rangle$ oscillate rapidly at the frequencies $+2\mathcal{E}$ and $-2\mathcal{E}$. Dropping these terms removes all interferences except the one between $|u,L\rangle$ and $|l,U\rangle$. This, also, is negligible because independent-atom scattering dominates—because coherence between $|u,L\rangle$ and $|l,U\rangle$ is only created when a count is recorded at detector A. Thus we obtain

$$\begin{aligned} 4I_c(x,t) = {} & [\Theta_{u,U}(t) + \Theta_{l,L}(t)](2 + |1 + e^{-i\theta}|^2) \\ & + [\Theta_{u,L}(t) + \Theta_{l,U}(t)](2 + |1 - e^{-i\theta}|^2), \end{aligned} \qquad (9)$$

where the subscripts refer to the *initial* state of the atoms, now a definite dressed state—$\Theta_{\delta,\Delta}(t) = 1$ when $|\psi_c(t)\rangle = |\delta,\Delta\rangle$ and zero otherwise.

The 12 possible transitions in the internal state of the atoms, given that a photon is recorded at detector A, are identified in Eq. (9) as follows: At each instant, one of the four functions $\Theta_{\delta,\Delta}(t)$ is unity and the others are all zero. For each of the four possibilities three different transitions can occur; for example, when $\Theta_{u,U}(t) = 1$ the transitions $|u, U\rangle \rightarrow |u, U\rangle$, $|u, U\rangle \rightarrow |l, U\rangle$, and $|u, U\rangle \rightarrow |u, L\rangle$ can occur. The terms $2 + |1 + e^{-i\theta}|^2$ and $2 + |1 - e^{-i\theta}|^2$, which multiply the $\Theta_{\delta,\Delta}(t)$ in Eq. (9), are proportional to the counting rates at detector A due to the three transitions. They are derived by working forward from Eq. (8) to Eq. (9). The derivation unambiguously assigns a rate to each individual transition—$|1 + e^{-i\theta}|^2$ to the transitions $|u, U\rangle \rightarrow |u, U\rangle$ and $|l, L\rangle \rightarrow |l, L\rangle$; $|1 - e^{-i\theta}|^2$ to the transitions $|u, L\rangle \rightarrow |u, L\rangle$ and $|l, U\rangle \rightarrow |l, U\rangle$; $1/2$ to each of the remaining transitions. This association between counting rates and transitions is of central importance. From it we see that detector A actually records three fringes, one on top of the other, each correlated with a particular change in the internal state of the atoms: (I) a 100% visibility fringe with maximum at $\theta = 0$ correlated with $|u, U\rangle \rightarrow |u, U\rangle$ or $|l, L\rangle \rightarrow |l, L\rangle$; (II) a 100% visibility fringe with maximum at $\theta = \pi$ correlated with $|u, L\rangle \rightarrow |u, L\rangle$ or $|l, U\rangle \rightarrow |l, U\rangle$; (III) a zero visibility fringe correlated with the remaining transitions, *all of which change the internal state of the atoms*. There are then two reasons why the net visibility is zero: (i) the 100% visibility fringes of classes I and II cancel, and (ii) the fringe of class III must have zero visibility because *which-path information is available by monitoring the change in the internal (dressed) state of the atoms*.

To conclude we show how the internal state of the atoms might be monitored, allowing the counting record at detector A to be sorted and the separate fringes to be recovered. Our scheme uses the cavity mode as a QND detector of the collective dressed-state inversion

$$M(t) = \langle\psi_c(t)|(\hat{u} - \hat{l} + \hat{U} - \hat{L})|\psi_c(t)\rangle/2\,; \qquad (10)$$

$M(t) = +1$, 0, and -1 when $|\psi_c(t)\rangle$ is $|u, U\rangle$, $|u, L\rangle$ or $|l, U\rangle$, and $|l, L\rangle$, respectively. Equation (7) shows that $M(t)$ is equal to the conditioned Y-quadrature amplitude of the collective atomic dipole. It is therefore correlated with the amplitude of the field radiated into the cavity and can be measured by homodyne detection of the field amplitude $Y(t) = i\langle\psi_c(t)|(\hat{a} - \hat{a}^\dagger)|\psi_c(t)\rangle$ at detector B. Under strong-coupling conditions ($g > \kappa > \gamma_I$) the scheme works as an analog of a spin-1 Stern-Gerlach apparatus, where spin flips occur each time a class III scattering event takes place. [Note that the results of Fig. 2 do not require the strong-coupling limit. The phase selection of Eq. (6) may, however, be applied in this limit, where it rejects all scattering events with initial state $|u, L\rangle$ or $|l, U\rangle$ and hence recovers a 50% visibility in the strongly saturated regime.]

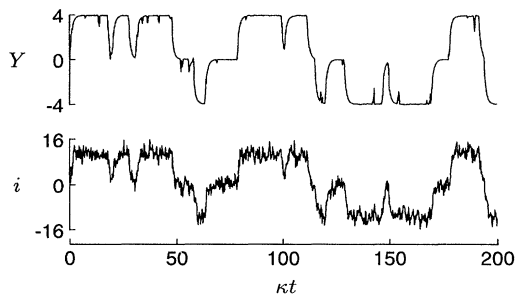

FIG. 5. A quantum trajectory illustrating the QND detection of the collective inversion for $\mathcal{E}/\gamma_I = 100$, $\gamma_I/\kappa = 0.2$, and $g/\kappa = 4$. The detection bandwidth is $\Gamma/\kappa = 5.0$.

The quantum trajectory analysis of the Stern-Gerlach analog is described elsewhere [5]. Its application to the present situation is illustrated by Fig. 5. The figure shows $Y(t)$, and the corresponding photocurrent $i(t)$ recorded by a finite bandwidth homodyne detector. The switching between dressed states appears in both. Each switch identifies a class III scattering event. Scattering events of classes I and II do not initiate a switch and cannot be identified in $i(t)$; although they are evident in $Y(t)$ as spikes marking the brief periods of decoherence which "decide" the class of each scattering event. (Note that Fig. 5 was produced without making the secular approximation. The realization of a distinct type for each scattering event is therefore a dynamical consequence of the measurement model; it is not inserted by hand.)

By correlating the counts at detector A with the record $i(t)$, the fringes of classes I, II, and III can be separately displayed. With regard to the class III fringe, in this scheme $i(t)$ does not, in fact, provide which-path information; it merely identifies the scattering events for which this information is, in principle, available. To actually obtain the which-path information one might use two cavities, one coupled to each of the atoms. The analog is then with two spin-1/2 Stern-Gerlach apparatuses. Each spin flip is recorded by one apparatus and not the other, and hence is assigned to a particular atom.

This work was supported by NSF under Grants No. PHY-9214501 and No. PHY-9301571. M. G. R. acknowledges support from the Alfred P. Sloan Foundation.

[1] J. D. Cresser *et al.*, in *Dissipative Systems in Quantum Optics*, edited by R. Bonifacio (Springer, Berlin, 1982), pp. 21–59.
[2] M. G. Raizen *et al.*, Phys. Rev. A **45**, 6493 (1992).
[3] U. Eichmann *et al.*, Phys. Rev. Lett. **70**, 2359 (1993).
[4] H. J. Carmichael, *An Open Systems Approach to Quantum Optics*, Lecture Notes in Physics Vol. M18 (Springer, Berlin, 1993).
[5] H. J. Carmichael, P. Kochan, and L. Tian, in *Coherent States: Past, Present, and Future*, edited by D. H. Feng, J. R. Klauder, and M. R. Strayer (World Scientific, Singapore, 1994), pp. 75–92.